THE JOURNAL OF BIOLOGICAL CHEMISTRY
Vol. 277, No. 7, Issue of February 15, pp. 5351–5359, 2002

Printed in U.S.A.

A Mutational Analysis of the Globotriaosylceramide-binding Sites of Verotoxin VT1*

Received for publication, August 4, 2001, and in revised form, November 7, 2001
Published, JBC Papers in Press, November 26, 2001, DOI 10.1074/jbc.M107472200

Anna M. Soltyk‡§, C. Roger MacKenzie¶, Vince M. Wolski‡§, Tomoko Hirama¶, Pavel I. Kitov‖, David R. Bundle‖, and James L. Brunton‡§‡‡**

*From the ‡Clinical Science Division, University of Toronto, Toronto, Ontario M5S 1A8, Canada, the §Samuel Lunenfeld Research Institute, Mount Sinai Hospital, Toronto, Ontario M5G 1X5, Canada, the ¶Institute for Biological Sciences, National Research Council of Canada, Ottawa, Ontario K1A 0R6, Canada, the ‖Department of Chemistry, University of Alberta, Edmonton, Alberta T6G 2G2, Canada, and the **Toronto General Hospital, Toronto, Ontario M5G 2C4, Canada*

***Escherichia coli* verotoxin, also known as Shiga-like toxin, binds to eukaryotic cell membranes via the glycolipid Gb_3 receptors which present the P^k trisaccharide Galα(1–4)Galβ(1–4)Glcβ. Crystallographic studies have identified three P^k trisaccharide (P^k-glycoside) binding sites per verotoxin 1B subunit (VT1B) monomer while NMR studies have identified binding of P^k-glycoside only at site 2. To understand the basis for this difference, we studied binding of wild type VT1B and VT1B mutants, defective at one or more of the three sites, to P^k-glycoside and pentavalent P^k trisaccharide (pentaSTARFISH) in solution and Gb_3 presented on liposomal membranes using surface plasmon resonance. Site 2 was the key site in terms of free trisaccharide binding since mutants altered at sites 1 and 3 bound this ligand with wild type affinity. However, effective binding of the pentaSTARFISH molecule also required a functional site 3, suggesting that site 3 promotes pentavalent binding of linked trisaccharides at site 1 and site 2. Optimal binding to membrane-associated Gb_3 involved all three sites. Binding of all single site mutants to liposomal Gb_3 was weaker than wild type VT1B binding. Site 3 mutants behaved as if they had reduced ability to enter into high avidity interactions with Gb_3 in the membrane context. Double mutants at site 1/site 3 and site 2/site 3 were completely inactive in terms of binding to liposomal Gb_3, even though the site 1/site 3 mutant bound trisaccharide with almost wild type affinity. Thus site 2 alone is not sufficient to confer high avidity binding to membrane-localized Gb_3. Cytotoxic activity paralleled membrane glycolipid binding. Our data show that the interaction of verotoxin with the Gb_3 trisaccharide is highly context dependent and that a membrane environment is required for biologically relevant studies of the interaction.**

Verotoxins produced by *Escherichia coli* have been associated with diarrhea, hemorrhagic colitis, and the hemolytic uremic syndrome in humans (1, 2). There is evidence that verotoxins play a central role in the pathogenesis of these diseases, causing microvascular damage by direct toxicity to endothelial cells. Verotoxins consist of an enzymatic A subunit (32 kDa) that is noncovalently associated with a homopentameric receptor-binding B subunit (37.5 kDa). After holotoxin internalization by the cell, the A subunit causes catalytic inactivation of the 28 S ribosomal RNA, disrupting protein synthesis and inducing apoptosis (3, 4). Receptor binding is the primary event leading to toxin internalization, which is required for cellular toxicity (5).

The B subunit oligomer is responsible for toxin binding to the carbohydrate portion of the specific cell-surface glycolipid receptor and it has been shown that the susceptibility to VT1 toxin is correlated with Gb_3[1] receptor presence on the cell surface (6). In the absence of the A subunit, B subunit monomers form pentamers that are fully functional in terms of binding to Gb_3 (7). Determination of the crystal structure of the B pentamer in both the native form (8) and in complex with a P^k trisaccharide receptor analogue (9) identified three receptor-binding sites per B subunit monomer (Ref. 9, Fig. 1*A*). Site 1, located at the cleft between adjacent B subunits, is characterized by a hydrophobic stacking interaction of the Phe-30 phenyl ring with Galβ of the receptor and by hydrogen bonds involving Asp-17, Thr-21, Glu-28, and Gly-60. Site 2 is located on the opposite side of the phenyl ring of Phe-30 in a crevice defined by Gly-62, Asn-32, Arg-33, Asp-16, and Ala-56. Interaction with receptor oligosaccharide at this site primarily involves hydrogen bonds. The third binding site involves hydrophobic stacking interaction of Galβ against the indole ring of Trp-34 and a hydrophobic interaction between Galα and Trp-34 of an adjacent monomer. In addition, Galα hydrogen bonds to Trp-34 and Asn-35 as well as Asp-18 from an adjacent monomer. The solution structure of VT1 in the absence (10) and presence of a Galα(1–4)Galβ(1–4)Glcβ1-O-trimethylsilylethyl analogue of Gb_3 (11) and the P^k trisaccharide (12) has been determined by isotope assisted NMR techniques. At equimolar concentrations of P^k trisaccharide and B subunit monomer, only site 2 was significantly occupied with the receptor analogue. Detection of VT1B·P^k-glycoside complexes by Fourier transform ion cyclotron resonance mass spectrometry confirmed and extended the NMR data (13). By observing VT1B·P^k trisaccharide complexes for increasing ratios of oligosaccharide to VT1B the distribution of bound species could be studied.

* This work was supported by Grant FRN 13071 from the Canadian Institutes of Health Research (to J. L. B.). This is National Research Council of Canada Publication 42448. The costs of publication of this article were defrayed in part by the payment of page charges. This article must therefore be hereby marked "*advertisement*" in accordance with 18 U.S.C. Section 1734 solely to indicate this fact.

‡‡ To whom correspondence should be addressed: Dept. of Microbiology, The Toronto General Hospital, 200 Elizabeth St., Norman Urquhart Wing, 13th floor, Rm. 122, Toronto, Ontario M5G 2C4, Canada. Tel.: 416-340-3183; Fax: 416-340-5047; E-mail: james.brunton@uhn.on.ca.

[1] The abbreviations used are: Gb_3, globotriaosylceramide (Galα(1–4)Galβ(1–4)Glcβ-Cer); RU, response unit; P^k trisaccharide, [Galα(1–4)Galβ(1–4)Glcβ]; P^k-glycoside, the trimethylsiylethyl derivative of the P^k trisaccharide; SPR, surface plasmon resonance; TLC, thin-layer chromatography; VT1, verotoxin-1, VT1B, the pentameric B subunit of verotoxin 1.

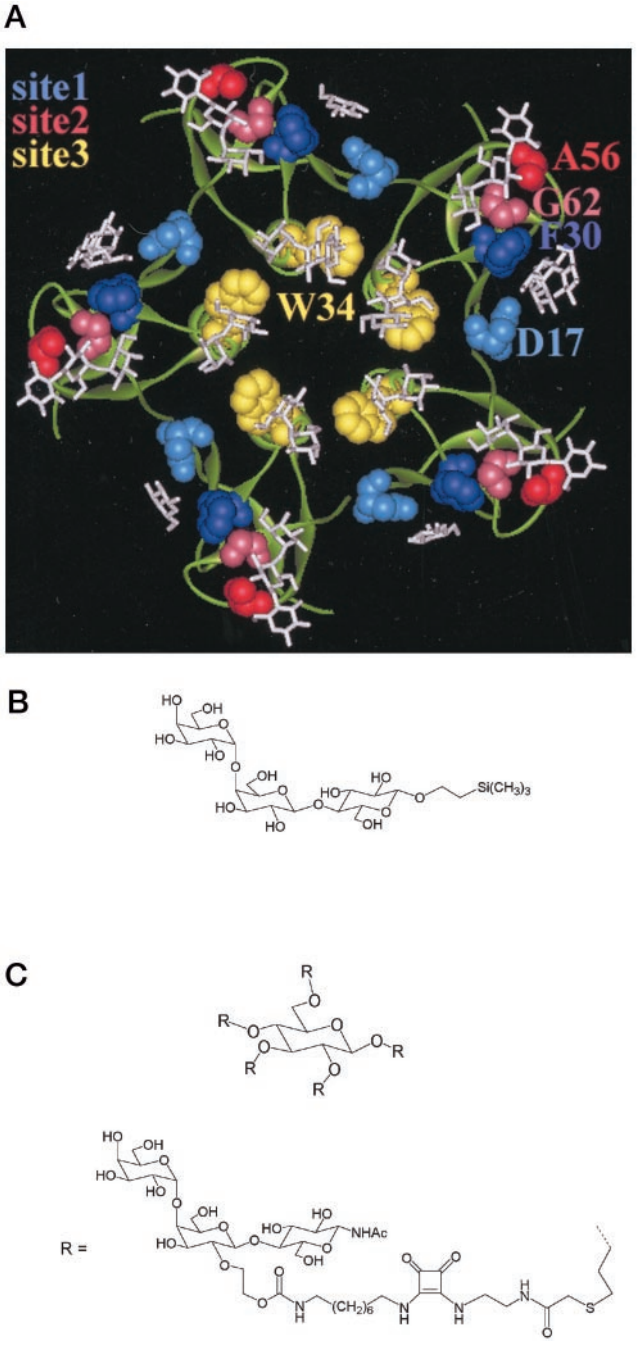

FIG. 1. **Molecular structure of VT1B subunit, P^k-glycoside, and pentavalent STARFISH.** *A,* model of the B subunit in interaction with P^k trisaccharide was produced with the WebLab ViewerPro program from x-ray crystallographic coordinates obtained from the Brookhaven Protein Data Base (PDB ID 1BOS, Ref. 9). The side interacting with the membrane receptor is shown. Note that the electron density map of bound carbohydrates defined all three P^k-glycoside rings at all site 2 pockets but only some sites 1 and 3 pockets (9). Amino acids discussed in this paper are indicated in a monomer where all sugar rings were defined: Phe-30 and Asp-17 belong to site 1 (*dark* and *light blue*), Ala-56 and Gly-62 to site 2 (*dark* and *light red*), and Trp-34 represents site 3 (*yellow*). *B,* molecular structure of P^k-glycoside used in SPR experiments. *C,* molecular model of pentavalent STARFISH. The *dotted line* represents the bond between the R group and the ring oxygen atoms of the glucose core.

With the B subunits associating into a pentameric doughnut-shaped structure and each monomer exhibiting three binding sites, the VT1 molecule contains a total of 15 saccharide-binding sites aligned on one face. The interaction of the B-subunit pentamer with P^k-glycoside is not very strong (K_d in a millimolar range) and the efficient binding of the B pentamer to membrane glycolipid is due to multivalent interaction. A decavalent model receptor-inhibitor molecule STARFISH was described recently and shown to have an *in vitro* inhibitory activity 1–10 million-fold higher than univalent ligands (14). It is by far the highest molar activity of any inhibitor yet reported for VT1 and VT2. Since decavalent STARFISH was shown to interact simultaneously with two B subunit pentamers (14), we synthesized a new but related, pentavalent STARFISH (pentaSTARFISH) molecule (Fig. 1*C*). PentaSTARFISH is built from five P^k-glycosides substituted by a tether at *O*-2 of the central galactose residue attaching each P^k unit to the central glucose core, resulting in a five-ray cluster of P^k units.

We previously reported data on the binding of VT1B subunit mutants designed to specifically inactivate individual sites. All three sites identified by crystallography appeared to be biologically relevant and blockage of sites 1 and 2 resulted in the most significant reduction of binding and cytotoxicity (15). To better define the biological significance of the three binding sites, we constructed additional mutants, including double site mutants designed to elucidate the function of individual sites. The interaction of mutated B subunits with monovalent and pentavalent forms of the carbohydrate portion of Gb_3, the P^k trisaccharide, was analyzed in real time by surface plasmon resonance. The effect of these mutations on B pentamer binding to membrane receptor was monitored by SPR using a liposome capture technique (16). In this technique glycolipid receptor is incorporated into artificial liposomes that also contain a small amount of lipopolysaccharide (LPS), allowing the capture of these liposomes on SPR sensor chip surfaces via an immobilized anti-LPS monoclonal antibody. This method provides a better approach to the study of protein-glycolipid interactions than conventional microtiter plate or TLC overlay methods because it better mimics the membrane environment. In addition, the cytotoxic activity and intracellular routing of the corresponding mutant holotoxins were correlated with cell surface binding as determined by flow cytometry.

EXPERIMENTAL PROCEDURES

Materials—All restriction enzymes, DNA polymerase I, calf intestinal polynucleotide kinase, T4 DNA ligase, RNase A, and dNTPs were purchased from Amersham Bioscience, Inc. Ampicillin, kanamycin, polymyxin B sulfate, and isopropyl-β-D-thiogalactoside were purchased from Sigma. Oligonucleotides used for mutagenesis were purchased from Dalton Chemical Laboratories Inc. [^{35}S]dATP for sequencing was purchased from PerkinElmer Life Sciences. Human renal Gb_3 and monoclonal antibody PH1, specific for VT1B subunit (17), were obtained from Dr. C. Lingwood, The Hospital for Sick Children, Toronto, ON. Monoclonal antibodies 13C4, 16E6, and 19G8 (18, 19) were kindly provided by Dr. A. D. O'Brien, Uniformed Services University of the Health Sciences, Bethesda, MD.

Monovalent and Pentavalent P^k Trisaccharide Synthesis—The monovalent form of the P^k trisaccharide (P^k-glycoside, Fig. 1*B*), was synthesized as described previously (20). The pentavalent STARFISH (Fig. 1*C*) form of the P^k trisaccharide was synthesized by a method that will be described elsewhere.[2]

Bacterial Strains—*E. coli* DH5α F′Φ80ΔlacZΔM15Δ(lacZYA-argF) U169*end*A1*rec*A1*hsd*R17($r_K^-mK^+$)*deo*R*thi*-1*sup*E44λ-*gyr*A96*rel*A1 (Invitrogen) was used for all plasmid preparations for DNA sequencing and cloning. *E. coli* JM101 F′ *tra*D36 *pro*A$^+$ *pro*B$^+$ *lac*I^q *lac*ZΔM15 *sup*E *thi*/F′ Δ(*lac-pro*AB) (21) was used for expression of all B subunit and holotoxin mutants. *E. coli* BW313 *Hfr lysA*$^-$ *dut ung thi-1 recA spoT1* (22) was used for preparation of uracil-containing single stranded DNA for site-directed mutagenesis.

Site-directed Mutants—Oligonucleotide-directed site-specific mutagenesis was performed as previously described (15, 22). Multiple mutations were introduced, one at a time, in the same manner. The following mutagenic oligonucleotides were used: D17E, TATAATGATGAAGATACCTTT; F30A, GAATTAGCGACCAACAGATG; A56Y, AAA-

[2] P. I. Kitov and D. R. Bundle, submitted for publication.

CTAATTACTGTCATAATG; G62A, GGAGGGGCATTCAGCGAAG; G62T, GGAGGGACATTCAGCGAAG; W34A, CAACAGAGCGAATCTTCAGT. Mutant holotoxin expression plasmids were made by subcloning the *Acc*I 439-bp restriction fragment carrying each of the B subunit mutations into the wild type toxin expression vector pJLB128 (23). The presence of the mutations was confirmed by double strand sequencing using the Sequenase 2.0 sequencing kit (U. S. Biochemical Corp.). Wild type and mutant B pentamers and holotoxins were expressed and purified (24, 25). All of the mutant B pentamers and holotoxins were characterized by denaturing and native polyacrylamide gel electrophoresis to confirm protein integrity. The structural integrity of mutant B pentamer and holotoxin molecules was confirmed by demonstration of reactivity with a panel of monoclonal antibodies specific for B pentamer epitopes (19). To demonstrate that the mutant B subunits were capable of pentamerization, subunit cross-linking was performed using dimethyl suberimidate (26). Swiss PDB Viewer OpenGL 3.51, obtained from the ExPaSy Internet page (www.expasy.ch), was applied to model VT1B subunit mutants. The crystal structure of VT1 B subunit from Protein Data Bank file (1bov) was used (www.rcsb.org/pdb).

Surface Plasmon Resonance—Analyses were performed using a BIACORE 1000 and 3000 biosensor systems (27). Varying amounts of Gb_3 were incorporated into liposomes that also contained dimyristoylphosphatidylcholine and *Salmonella* serogroup B LPS. A monoclonal antibody specific for the *Salmonella* LPS and immobilized on research grade CM5 sensor chips (Biacore, Inc.) served as a capture molecule for the liposomes (16). The antibody-LPS interaction retained the liposomes on sensor chips with no detectable dissociation, thereby providing a stable surface for VT1B binding.

Following the capture of ~1000 RUs of liposomes, holotoxin, or B pentamer were injected over the liposome surfaces. Reference surfaces were prepared using liposomes containing only dimyristoylphosphatidylcholine and LPS. All analyses were carried out in 10 mM HEPES, pH 7.4, containing 150 mM NaCl and 3.4 mM EDTA, at 25 °C and a flow rate of 10 μl/min. The antibody surfaces were regenerated with sequential 3-s injections of 1 and 4 mM sodium taurodeoxycholate in 10 mM sodium acetate buffer, pH 4.5. For the measurement of P^k-glycoside and pentaSTARFISH binding to VT1B, wild type and mutant toxins were immobilized on CM5 sensor chips by amine coupling at pH 4.5 to give surface densities of ~4000 RUs. Analyses were performed in the above buffer at 25 °C and a flow rate of 40 μl/min. The triple site mutant, F30A/G62T/W34A, was used as a reference surface. Surface regeneration was not necessary. Data were evaluated using the BIAevaluation 3.0 software (Biacore, Inc.).

Thin-layer chromatography (TLC) overlay assays were performed as described earlier (28) using Polygram SIL G or Alugram Nano-Sil G/UV_{254} thin layer silica plates (Macherey-Nagel Duren) and 3-fold serial dilutions of wild type and mutant B pentamers. Toxin binding was detected with antibody PH1.

Cell Culture—African green monkey kidney Vero 76 cells and human Burkitt's lymphoma Daudi cells were purchased from the American Type Culture Collection. Human monocyte THP1 cells were provided by Dr. O. Rotstein, University of Toronto. The cells were grown at 37 °C in 5% CO_2 in RPMI 1640 medium supplemented with 0.1% glutamine, 100 units/ml penicillin, 0.1 mg/ml streptomycin (Invitrogen), and 10% heat-inactivated fetal bovine serum (CanSera).

Quantitation of VT1B Binding to Cells in Culture—FITC labeling of VT1B pentamers was performed as earlier described (29). The efficiency of FITC incorporation into individual mutants was very similar in all instances as judged from the fluorescence intensity of serially diluted samples run on polyacrylamide gels. Toxin binding to Vero cells was quantitated by fluorescence-activated cell sorting. Vero cells were trypsinized and washed with complete medium containing 10% fetal calf serum. Approximately 10^6 cells were incubated in medium containing 10 μg/ml FITC-labeled mutant B subunit at 4 °C for 1 h. Cells were washed by pelleting and resuspended in phosphate-buffered saline supplemented with 1 mM EDTA and fixed in 1% paraformaldehyde prior to fluorescence-activated cell sorting analysis. Mutant toxin binding was expressed as a percent of wild type toxin binding. Trendlines and standard errors were calculated using Microsoft Excel.

Cytotoxicity Assays and Immunocytochemistry—The toxicity of purified wild type and mutant holotoxins was determined as previously described (15). For imunocytochemistry, wild type and mutant VT1B subunits were conjugated with Texas Red-X or Oregon Green 488, respectively, using FluoroReporter Labeling Kits (Molecular Probes) according to the manufacturers protocol. The efficiency of fluorescence incorporation into individual mutants was very similar as judged from the fluorescence intensity of serially diluted samples run on polyacrylamide gels and by spectroscopy. To compensate for much lower binding of mutant toxins and to obtain similar intensities of fluorescence from mutant and wild type toxin during internalization, we used higher molar ratio of dye to protein (MR) for Oregon Green 488 (RM = 20) than for Texas Red labeling (RM = 5). To determine the relationship between toxin binding and cytotoxicity, the data were log transformed and general linear models were created using SAS and Splus, using data for the A56Y, D17E, F30A, and G62A mutants. Standard deviations were calculated using Microsoft Excel. Internalization of fluorescent VT1B subunits in Vero cells was done as described earlier (30). Analysis of samples was performed using the ×100 objective of an Olympus 1X-70 inverted microscope equipped with fluorescence optics and Deltavision Deconvolution Microscopy software (Applied Precision). Digital images were processed in Adobe Photoshop (Adobe Systems).

TABLE I
Site-directed VT1 mutants and their cytotoxicity

Mutation(s)	Affected site(s)[a]	Cytotoxicity	
		CD_{50}[b]	Fold reduction
		ng/ml	
Wild type		0.0061 ± 0.0018	1
F30A	1	1,100 ± 600	10^5
D17E	1	6.7 ± 3.2	10^3
A56Y	2	1.4 ± 1	10^2
G62T	2	10,000 ± 2,500	10^6
G62A	2	1,900 ± 820	10^5
W34A	3	0.046 ± 0.002	10
F30A/G62T	1, 2	360,000 ± 100,000	10^8
F30A/W34A	1, 3	3,300 ± 510	10^5
D17E/W34A	1, 3	3,300 ± 10	10^5
A56Y/W34A	2, 3	3,300 ± 510	10^5
G62T/W34A	2, 3	11,000 ± 3,200	10^6
F30A/G62T/W34A	1, 2, 3	740,000 ± 55,000	10^8

[a] Sites are designated according to Ling *et al.* (9).
[b] Cytotoxicity is expressed as an average of at least three independent experiments ± S.E.

RESULTS

Design of Holotoxin and B-pentamer Mutants—The series of mutants designed to selectively eliminate ligand binding at sites 1, 2, 3, or combinations thereof is described in Table I. Two site 1 mutants (D17E and F30A), one site 2 mutant (G62T), and one site 3 mutant (W34A) were previously described and studied for Gb_3 binding (in a lipid milieu in microtiter plates) and cytotoxicity (15, 25). As part of the present study, several additional mutants were made in an effort to further clarify the biological significance of the three Gb_3-binding sites. Attention was turned to improving the specificity of mutants designed to block binding at site 2. The previously reported substitution G62T, designed to sterically block site 2, was shown to cause a shift of the Phe-30 phenyl ring into site 1, the magnitude of which was dependent on the conformation of the threonine side chain. This suggested that binding at both sites 1 and 2 might be affected (15). The mutant G62A was produced to eliminate binding at site 2 while having less effect on site 1. Modeling, however, suggested that the presence of a β-carbon at residue 62 would still have a small effect on the phenyl ring of Phe-30, a key residue of site 1[3] (15). Because of the proximity of key residues involved in sites 1 and 2, we produced another mutant altered at a location more distant from site 1. The substitution A56Y was chosen since the methyl group of Ala-56 had previously been shown to interact with the trisaccharide bound at site 2 (9, 11). Mutants D17E/W34A and F30A/W34A were intended to disrupt sites 1 and 3 while leaving site 2 intact. Similarly, mutants G62T/W34A and A56Y/W34A were intended to disrupt sites 2 and 3 while leaving site 1 intact although, as noted above, site 1 is affected by the G62T mutation. Mutant F30A/G62T was designed to simultaneously disrupt site 1 and site 2, leaving only site 3 functional, while the

[3] R. J. Read, unpublished observations.

TABLE II
Affinities of the binding of P^k-glycoside and pentavalent STARFISH to wild type and mutant VT1Bs

Mutation(s)	Site(s)[a]	P^k-glycoside K_D[b]	Pentavalent STARFISH K_D[b]
		M	
Wild type		4.8×10^{-3} (7.3%)	1.7×10^{-8} (6.8%)
D17E	1	7.5×10^{-3} (9.4%)	8.0×10^{-7}[c] (4.3%)
F30A	1	1.2×10^{-2} (6.7%)	4.0×10^{-7}[c] (5.7%)
A56Y	2	No binding	1.6×10^{-5}[c] (2.1%)
G62A	2	No binding	1.3×10^{-5}[c] (7.1%)
W34A	3	5.0×10^{-3} (6.2%)	2.0×10^{-5}[c] (6.5%)
D17E/W34A	1, 3	9.9×10^{-3} (7.0%)	1.1×10^{-5}[c] (7.3%)
A56Y/W34A	2, 3	No binding	9.8×10^{-4} (4.7%)[c]

[a] Sites are designated according to Ling *et al.* (9).
[b] Numbers in parentheses are standard errors for linear fitting of equilibrium RU/concentration *vs* equilibrium RU (95% confidence limits).
[c] Highest affinity component of mixed binding (see Fig. 2*F*).

triple mutant F30A/G62T/W34A was expected to eliminate binding completely.

Analysis of Mutant B Subunit Proteins—The immunoreactivities of purified mutant and wild type B subunits were compared using a panel of monoclonal antibodies (PH1, 13C4, 16E6, and 19G8) that recognize conformational epitopes on VT1B. All the mutant and wild type B subunits reacted equally well with PH1 and 13C4 monoclonal antibodies. The 16E6 antibody exhibited less efficient recognition of all the W34A mutants (W34A, D17E/W34A, and F30A/W34A) relative to the wild type, while reacting normally with mutants D17E and F30A. The 19G8 antibody bound all the B pentamers equally well except for the G62T mutants. Since x-ray crystallography of the W34A and G62T mutant B pentamers showed normal protein folding (38), we concluded that the lower reactivity of these mutants toward 16E6 and 19G8, respectively, was indicative of contributions by Trp-34 and Gly-62 to the epitopes recognized by these antibodies and not of improper folding. SDS-PAGE analysis of dimethyl suberimidate cross-linked products of all mutant B subunits yielded results identical to the wild type, indicating that the mutations did not alter B subunit pentamer formation (data not shown).

P^k-glycoside and Pentavalent STARFISH Binding to VT1B—Only mutants with an intact site 2 were capable of binding P^k-glycoside at levels that were detectable (Table II). Despite the low affinity of the monovalent interaction, sufficient levels of binding were obtained for the determination of K_D values by Scatchard analysis (Fig. 2, *A* and *B*). With a K_D of ~5 mM, the monovalent binding of P^k-glycoside was 5×10^7 times weaker that the multivalent binding of wild type toxin to liposomal Gb_3 (see below). The P^k-glycoside data also indicated that site 2 was completely unaffected by the W34A mutation at site 3 and only very slightly affected by the D17E at site 1, while there was a greater reduction in site 2 binding with F30A substitution at site 1.

The binding characteristics of pentaSTARFISH were very different from those of P^k-glycoside in that the W34A mutation had a pronounced effect on pentaSTARFISH binding. The data for pentaSTARFISH binding to wild type VT1B gave exceptionally good global fitting to a 1:1 interaction model (Fig. 2*C*), indicating homogeneous pentavalent binding. The 1:1 fitting gave a $k_a = 9.8 \times 10^6$ M^{-1} s^{-1} and a $k_d = 0.16$ s^{-1}. These rate constants give a $K_D = 1.6 \times 10^{-8}$, which is the same as that obtained by Scatchard analysis of the equilibrium binding data (Fig. 2*D*, Table II). This affinity is 3×10^6 times that of the P^k-glycoside-VT1B interaction (Table II). Whereas the affinity of W34A for P^k-glycoside was identical to that of wild type VT1B, the affinity of W34A for pentaSTARFISH was over 1000-fold weaker than wild type VT1B- pentaSTARFISH interaction. Of the single site mutants W34A showed the lowest affinity for pentaSTARFISH (Table II). Site 2 mutants, for which P^k-glycoside binding could not be detected, did bind pentaSTARFISH with micromolar affinities (Table II). Scatchard analysis of the pentaSTARFISH equilibrium binding data for mutants, including W34A (Fig. 2, *E* and *F*), gave nonlinear plots.

VT1B Binding to Liposomal Gb_3—Surface plasmon resonance data collected for the binding of toxin to Gb_3 presented on liposomal surfaces provided kinetic and affinity data for the receptor binding properties of the various mutants relative to the wild type. The holotoxin and B pentamer forms of VT1 displayed similar binding kinetics and affinities when injected over liposomes containing Gb_3. A higher response was observed for the holotoxin because of its greater mass. In light of the similar binding profiles, all subsequent binding studies, with the exception of A56Y/W34A, were conducted using the B pentamer.

At a liposomal Gb_3 concentration of 2%, VT1B binding was biphasic, particularly in the dissociation phase (Fig. 3*A*). The existence of a rapid dissociation rate suggests that a significant proportion of the toxin molecules bound at low valency. Much better binding was observed at glycolipid concentrations of 5 and 10% (Fig. 3*A*). At a liposomal Gb_3 concentration of 10% and a wild type VT1B concentration of 40 nM, the binding data fit well to a 1:1 interaction model (Fig. 3*B*). This is presumed to indicate that homogeneity of binding at the maximum binding valency for the interaction is reached under these conditions. Good fits were observed for only a relatively narrow concentration range, one that presumably gives homogeneity with respect to binding valency. Based on the derived rate constants, the functional affinity of the interaction is ~1 nM (Table III) under these conditions.

The single site mutants all bound to liposomal Gb_3 but with varying levels of activity. With the exception of A56Y and W34A, the binding data for all site 1 and site 2 mutants fit reasonably well to a 1:1 interaction model; the fit for the F30A data is presented in Fig. 3*C*, as an example. One site 1 mutant (D17E) and one site 2 mutant (A56Y) exhibited binding strengths approaching that of the wild type (Fig. 3, *A*, *D*, and *E*), while a second site 1 mutant (F30A) and two other site 2 mutants (G62T and G62A) had much reduced binding activity relative to the wild type. The rate constants and functional affinities derived in this way indicated that D17E bound liposomal Gb_3 10-fold less efficiently than wild type VT1B and that F30A, G62T, and G62A were 100-fold less active than the wild type in this regard. The site 3 mutant (W34A) showed a much reduced level of binding to liposomal Gb_3 and a biphasic dissociation phase with the slower phase giving a rate constant almost identical to that of the wild type (Fig. 3*F*, Table III). The W34A data is consistent with two populations of bound molecules that differ with respect to occupancy of the two available sites 1 and 2.

With the exception of the double site 1/site 2 mutant (F30A/G62T), which showed very weak but detectable binding to liposomal receptor, all of the double site mutants were completely inactive in terms of glycolipid binding. This observation was particularly striking for the D17E/W34A and the A56Y/W34A double mutants since the single mutants D17E and A56Y exhibited relatively strong Gb3 binding activity. Moreover, the double mutant D17E/W34A showed no reduction in binding to the P^k trisaccharide in solution compared with the single mutant D17E (Table II).

In agreement with observations obtained by SPR, TLC overlay assays showed reduced binding of single mutant B pentam-

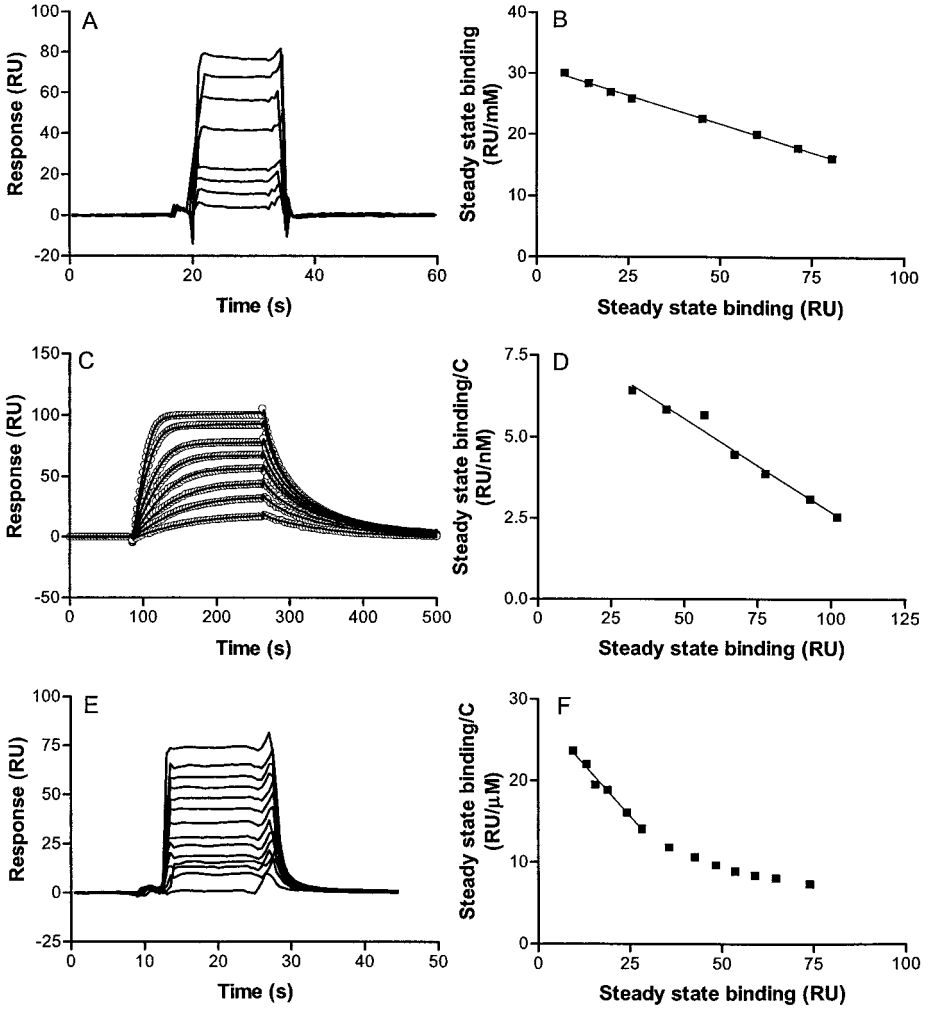

FIG. 2. **Binding of monovalent P^k-glycoside and pentavalent STARFISH to wild type and W34A VT1B.** Sensograms (*A, C*, and *E*) and Scatchard plots (*B, D*, and *F*) represent the interaction of P^k-glycoside (0.25–5 mM) with wild type VT1B (*A* and *B*), the interaction of pentaSTARFISH (2.5–40 nM) with wild type VT1B (*C* and *D*) and the interaction of pentaSTARFISH (0.1–10 μM) with W34A VT1B (*E* and *F*). The data for pentaSTARFISH binding to wild type VT1B was globally fitted to a 1:1 interaction model with the *open circles* representing the data points and the *solid lines* the global fit (*C*). *Error bars* are not shown on the Scatchard plots because replicate experiments were not always performed on surfaces with identical VT1B densities and capacities for oligosaccharide binding. Representative sensorgrams are shown in each instance.

ers F30A, D17E, G62T, and W34A to Gb_3 receptor immobilized in silica. Double mutations involving sites 1 and 3 (D17E/W34A and F30A/W34A) completely abolished *in vitro* binding of the B pentamer, while the double site 1/site 2 mutant (F30A/G62T) still bound detectably to Gb_3 (Fig. 4).

Binding of FITC-labeled B-pentamers and Cytotoxicity—The relative activities of wild type and mutant VT1B pentamers in terms of binding to Vero and THP-1 cells (Fig. 5) were very similar to those obtained by the SPR/liposome method. The A56Y, W34A, and D17E mutations reduced binding by 60–70, 75–90, and 90%, respectively. The correlation between the CD_{50} values of the mutant toxins and the amounts of B subunit bound to the cell surface, as measured by mean fluorescence intensity in fluorescence-activated cell sorting, was found to be logarithmic for most mutants with detectable binding (Fig. 6). The log transformed variables were linearly related ($y = 4840x^{-2.7}$, where $x = CD_{50}$, y = binding, $p < 0.004$). The W34A mutation was the exception in that it exhibited higher cytotoxicity than expected for the amount of bound toxin. The surface binding expressed as mean fluorescence intensity of the W34A and D17E mutants was similar: 55.5 ± 19.5 and 47.6 ± 15.1, respectively ($p = 0.609$). In contrast, the cytotoxicity of W34A was much greater than D17E (CD_{50} = 0.046 ± 0.02 and 6.7 ± 3 2, respectively, $p < 0.004$). The binding of all other mutants was less than 5% of that observed with the wild type B pentamer, and was not significantly different from background. The site 3 mutation W34A in combination with either site 1 or site 2 mutations (D17E/W34A, A56Y/W34A) resulted in 5×10^5 times lower toxicity than wild type. The G62A mutation of site 2 and the F30A mutation of site 1 both led to about a 10^5-fold decrease in cytotoxicity while the G62A mutant was 10 times more toxic than G62T. The site 1/site 2 (F30A/G62T) and site 1/site 2/site 3 (F30A/G62T/W34A) mutants exhibited toxicity only at the very high concentration of 1 mg/ml. At the same concentration, however, the B pentamer or heat-denatured holotoxin did not decrease cell viability (results not shown).

Routing of VT1B Mutants—We considered the possibility that elimination of some receptor-binding sites might alter the intracellular fate of internalized mutant holotoxin or B pentamer. Only wild type, D17E, A56Y, and W34A pentamers bound strongly enough to monitor VT1B routing by fluorescence microscopy. The kinetics of internalization and distribution for all three mutant B subunits were studied by simultaneous incubation of Oregon Green-conjugated wild type VT1B and Texas Red-conjugated VT1B mutants with Vero cells. The co-localization of A56Y and W34A with the wild type B subunit is shown in Fig. 7. The labeled pentamers were allowed to bind to Vero cells at 4 °C. At this temperature, the toxins were visible only at the cell surface (Fig. 7, *A* and *D*). In agreement with previously published data (30) and current understanding of retrograde transport, after warming the cells to 37 °C, internalization into a punctate vesicular compartment (endosomes) and a juxtanuclear region occurred within 15 min (Fig. 7, *B* and *E*) in all four instances. After an hour of incubation at 37 °C, most of the toxin accumulated around nuclei (Fig. 7, *C* and *F*) and this localization persisted through an overnight incubation (data not shown). The perinuclear structure containing VT1B was identified as the Golgi complex by co-labeling with antibodies

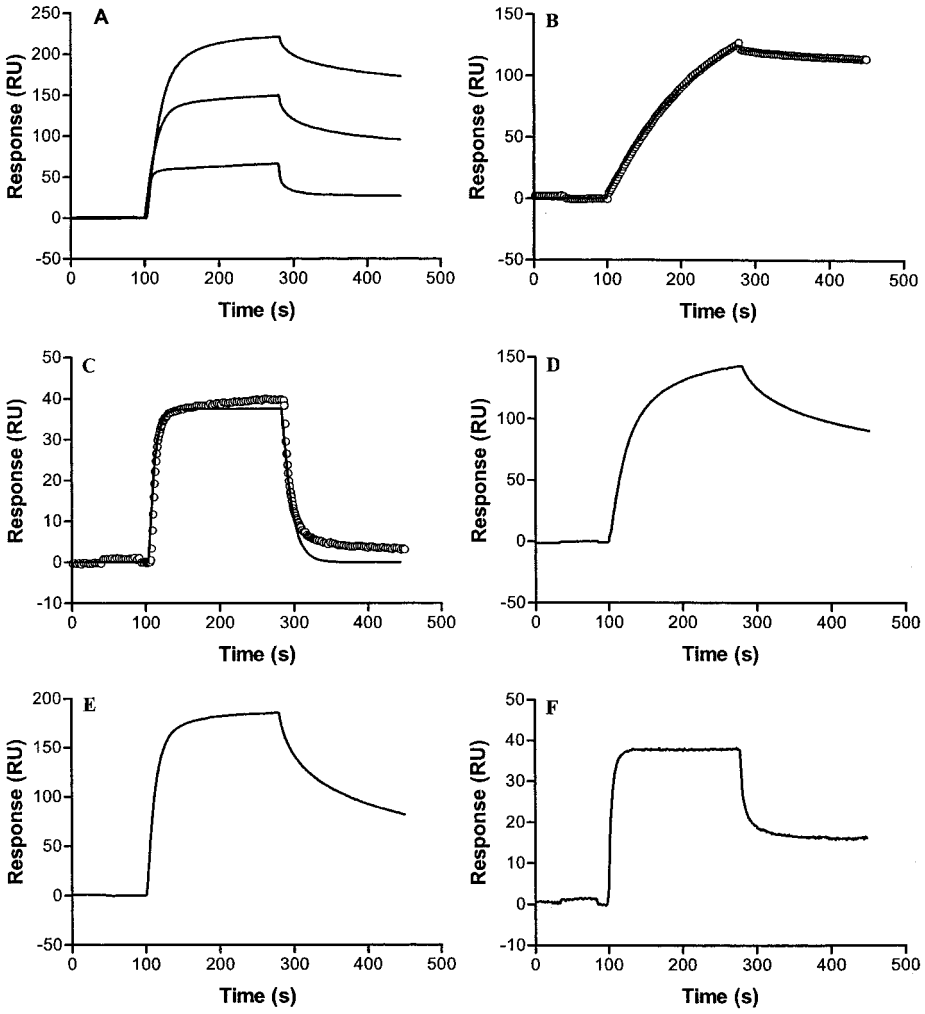

FIG. 3. **Real time binding data for the interaction of wild type and mutant VT1B pentamers with liposomal Gb_3.** *A,* binding of 150 nM wild type VT1B to liposomes containing 2% (*bottom*), 5% (*middle*), and 10% (*top*) Gb_3; *B,* fitting of the data for the binding of 40 nM wild type to liposomes containing 10% Gb_3 to a 1:1 interaction model; *C,* fitting of the data for the binding of 150 nM F30A to liposomes containing 10% Gb_3 to a 1:1 interaction model; *D,* binding of 150 nM D17E to liposomes containing 10% Gb_3; *E,* binding of A56Y to liposomes containing 10% Gb_3; *F,* binding of 150 nM W34A to liposomes containing 10% Gb_3. In *B* and *C* the *open circles* represent the data points and the solid lines the best fits to the model. Representative sensorgrams are shown in each instance.

TABLE III
Kinetic and affinity constants for the binding of wild type and mutant B pentamers to liposomes containing 10% Gb3

Mutation(s)	Site(s)[a]	k_a	k_d	K_D
		$M^{-1}\ s^{-1}$	s^{-1}	M
Wild type		2×10^5 (9.2%)[b]	6×10^{-4} (19%)	3×10^{-9} (16%)
F30A	1	3×10^5 (11%)	2×10^{-1} (2.8%)	7×10^{-7} (8.1%)
D17E	1	2×10^5 (11%)	2×10^{-3} (13%)	9×10^{-9} (16%)
A56Y	2		multiphasic association and dissociation	
G62T	2	3×10^5 (8.8%)	1×10^{-1} (4.4%)	4×10^{-7} (12%)
G62A	2	3×10^5 (14%)	4×10^{-2} (7.9%)	2×10^{-7} (25%)
W34A	3		1×10^{-3} (19%)[c]	

[a] Sites are designated according to Ling *et al.* (9).
[b] Numbers in parentheses are standard errors for fitting to a 1:1 interaction model (95% confidence limits).
[c] Slow dissociation phase in Fig. 3*F*.

against α-mannosidase, a resident of the medial- and trans-cisternae of the Golgi stack (data not shown).

DISCUSSION

B subunit binding to oligosaccharide presented as a membrane-bound glycolipid occurs in a very different context to that encountered in crystals, NMR experiments, and mass spectrometry studies which indicated a predominant role for site 2 (9, 11–13). In co-crystals, occupancy of all three sites was observed with the highest trisaccharide electron density at site 2 (38), while NMR experiments showed binding exclusively at site 2. Since the latter studies were performed at conditions of equimolar amounts of receptor analogue and B subunit monomer, the lower affinity sites may have been missed (11). However, mass spectrometry studies show that in the gas phase even at a P^k trisaccharide glycoside to B_5-homopentamer ratio of 63:1, the ligand occupies 5 sites with a K_D close to that of site 2 in solution, and only very small occupancy occurs for a sixth site, presumed to be site 1 (13). In the membrane, oligosaccharide presentation is constrained by the presence of the planar surface, and the conformation of the oligosaccharide may also be modulated by the Gb_3 lipid moiety (31, 32). In addition, the membrane receptor interaction is polyvalent, resulting in a high avidity interaction. To address these points, we studied the contribution of the three sites to the binding of monovalent and pentavalent forms of the P^k trisaccharide in solution and Gb_3 contained in liposomes. SPR allowed real time analysis of toxin binding and provided kinetic and affinity constants not

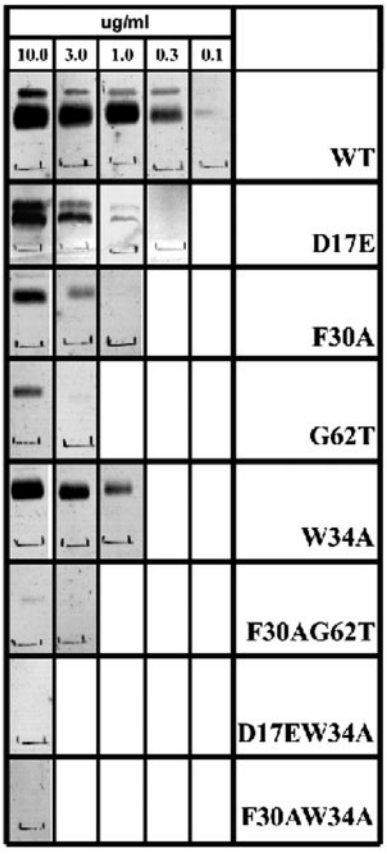

FIG. 4. **TLC overlays showing the binding of wild type and mutant VT1B pentamers to Gb_3.** Lanes containing 1 μg of renal Gb_3 were incubated overnight at room temperature in the presence of 10, 3, 1, or 0.3 μg of VT1B in PBS. Bound VT1B was detected as described under "Experimental Procedures."

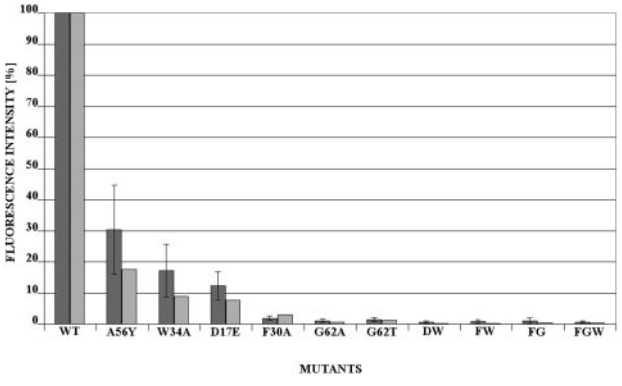

FIG. 5. **Quantitation of VT1B subunit binding to living cells in culture.** Vero or THP1 cells were exposed to FITC-labeled VT1B subunit mutants at 4 °C and analyzed by fluorescence-activated cell sorting. Mean fluorescence intensities, standardized for the fluorescence of control cells that were not exposed to fluorescent pentamer, were used as a measure of binding. These values were also standardized between experiments by expressing them as percentage of wild type toxin binding. The standard error was calculated from seven independent experiments performed with Vero cells (*dark gray*); the binding to THP1 cells (*light gray*) was measured only once. *WT*, wild type; *DW,* D17E/W34A; *FW,* F30A/W34A; *FG,* F30A/G62T; *FGW*, F30A/G62T/W34A.

previously available. Using an expanded panel of VT1B mutants, in combination with the real time analysis by SPR, we showed that all three P^k trisaccharide-binding sites identified by Ling *et al.* (9) play a role in toxin binding to membrane-associated Gb_3 and, therefore, are not artifacts associated with the crystal structure. The K_D for the interaction of wild type VT1B pentamer with Gb_3 incorporated into model membranes

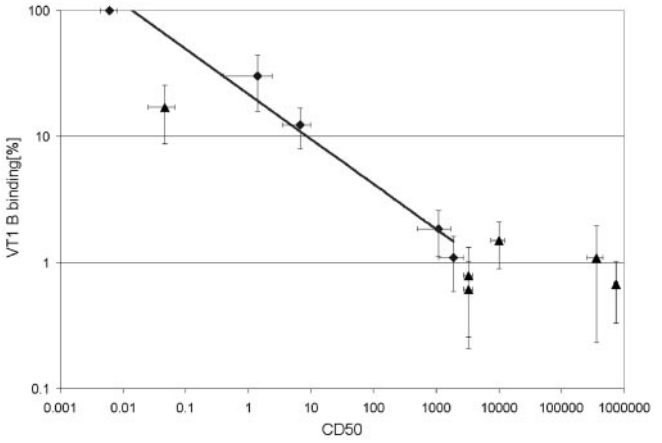

FIG. 6. **Correlation between toxicity and the binding of VT1B to Vero cells.** The fluorescence intensities resulting from binding of FITC-labeled B pentamers to Vero cells were plotted against the CD_{50} values obtained for the corresponding holotoxin. The points, from left to right are: wild type toxin, W34A, A56Y, D17E, F30A, G62A, D17E/W34A, F30A/W34A, G62T, F30A/G62T, and F30A/G62T/W34A. The *bars* represent standard errors from seven independent experiments. The trendline was calculated eliminating the points representing mutants carrying W34A mutations and mutants that exhibited the lowest binding.

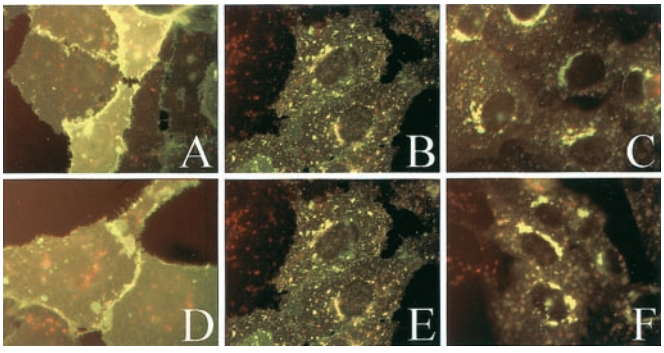

FIG. 7. **Co-localization of wild type, A56Y, and W34A VT1B subunits during internalization by Vero cells.** Cells were exposed to Oregon Green-labeled wild type VT1B together with Texas Red-labeled A56Y (*A-C*) or Texas Red-labeled W34A (*D* and *E*) B pentamers at 4 °C for 30 min (5 μg/ml of each) and washed with phosphate-buffered saline. VT1B internalization at 37 °C was monitored at 0 min (*A* and *D*), 15 min (*B* and *E*), and 60 min (*C* and *F*).

was over 10^7-fold higher than that for P^k trisaccharide and similar to the K_D reported for the binding of holotoxin to rabbit jejunal microvillus membranes (33) and in glycolipid-coated microtiter plate system (34). It is also similar to subnanomolar inhibitory activity observed for a decavalent P^k trisaccharide ligand that binds pentavalently to each of 2 VT1B molecules forming a 2:1 toxin-ligand complex (14). The kinetic K_D of 5 mM reported here for the P^k-glycoside-wild type VT1B interaction is slightly higher than the value of 1–2 mM determined by titration microcalorimetry (25) and nanoelectrospray mass spectrometry (13). In agreement with NMR studies (11, 12), our results indicated that the free P^k trisaccharide interaction is the strongest at site 2 and not detectable at sites 1 and 3, as mutations at the latter two sites had minimal or no measurable effect on binding of P^k-glycoside.

The data indicated a unique role for site 3. Although the W34A substitution did not affect the interaction between B subunit and P^k-glycoside, it did reduce the efficiency of B pentamer binding to membrane receptor. High affinity binding was still attained, only at a lower level and higher receptor concentration than for the wild type toxin. The profiles for the W34A mutant binding appeared identical to those observed for

the wild type at much lower receptor concentrations. These results suggest that site 3 promotes multivalent interactions between VT1 and the Gb_3 receptor. The interpretation of the role of site 3 in promoting multivalent interactions was confirmed by the dramatic effect of the W34A mutation on pentaSTARFISH binding. The observation that this substitution did not affect P^k-glycoside binding but reduced the affinity for pentaSTARFISH by over 3 orders of magnitude is very striking. The nonlinearity of the Scatchard plot for the W34A-pentaSTARFISH interaction (Fig. 2*F*) suggests varying degrees of site 2 occupancy, resulting overall in a lower valency interaction than for the wild type. We propose that functional site 3 aligns clustered or linked P^k trisaccharides, as on membranes and with pentaSTARFISH, to promote homogeneous pentavalent binding and to prevent random heterogenous cross-linking of B pentamers in the case of pentaSTARFISH. We propose that rapid and transient binding at site 3 precedes occupancy of the deeper potential energy wells at sites 1 and 2. This interpretation is consistent with a recent SPR study (35) of the binding of a related toxin, shiga toxin, to lipsomal glycolipid in which the existence of two binding sites per subunit monomer was proposed based on the finding that the data fit well to a bivalent analyte model. However, heterogeneous binding with respect to valency could also explain this result. The high K_D values reported by Nakajima *et al.* (35) suggest that maximum binding valency was not attained under their experimental conditions.

Analysis of binding of the mutants to P^k-glycoside together with molecular modeling has helped to clarify the specificity of the substitutions designed to affect each site. The idea that the mutant F30A is specific for site 1 as suggested in our previous study (15) must be reassessed in view of NMR evidence that the interaction with P^k trisaccharide occurs exclusively at site 2. Since microcalorimetry showed impaired binding of P^k trisaccharide to F30A in solution (25), we must assume that this reflects impaired binding at site 2. A likely explanation is the evidence of disorder in the glycine loop that forms the base of the site 2 pocket that was found in the NMR structure of the wild type (10, 11). Although disorder in this area was not found in the crystal structure of the wild type, further analysis of the crystal structure of the F30A B subunit has shown increased disorder in the same region compared with the wild type (39). Similarly, molecular modeling suggested that G62T probably impairs binding at site 1 as well as site 2. Molecular modeling also predicts that a small displacement of the phenyl ring of Phe-30 would be produced by a β carbon at residue 62, suggesting that G62A might still have an effect on site 1, albeit less that with the threonine substitution[3] (15). We therefore believe that the A56Y mutant produced in the present study results in a more specific impairment of site 2, while D17E is the most specific for site 1.

In the context of a lipid bilayer, both sites 1 and 2 are needed for strong binding. The SPR and cell toxicity data for mutants D17E and A56Y indicated a similar contribution of sites 1 and 2 to the avidity of the B pentamer for liposomal Gb_3. The role of Ala-56 in the interaction of site 2 with Gb_3 was previously observed by x-ray crystallography, and was supported by NMR studies (9, 11). The biological relevance of this residue has now been confirmed both by cytotoxicity and model membrane interaction. The double mutant studies unequivocally demonstrated the involvement of all three sites in binding to membrane Gb_3 and the importance of site 3. In the context of glycolipid, the double site 1/site 3 (D17E/W34A) and site 2/site 3 mutants (A56Y/W34A) were inactive with respect to receptor binding in both SPR and TLC formats. It was particularly striking that the W34A mutation in combination with the D17E or A56Y mutations, which singly were not very disruptive, completely abolished detectable binding to glycolipid while having virtually no effect on the interaction with P^k-glycoside. The crystal structures of the D17E/W34A·P^k complex, and the F30A/W34A·P^k complex show full occupancy at site 2 and none at sites 1 or 3 (38) but do not tell us much about the strength of the interaction. Our data suggest that the interaction of these mutants with P^k-glycoside is virtually identical to the wild type. Therefore we conclude that the presence of one high affinity site per B subunit monomer is not sufficient to produce high avidity binding of the pentamer to Gb_3 in the membrane context. This is important given previous publications suggesting that site 2 is the most important, and possibly sole, binding site (11, 12, 36).

There are still unresolved issues relating to the role of site 1 in VT1 binding to membrane Gb_3. While the affinity of site 2 for P^k-glycoside and pentaSTARFISH is clearly much higher than that of site 1, the liposomal data indicates that sites 1 and 2 make similar contributions in terms of binding to membrane Gb_3. For example, the site 1 mutant D17E and the site 2 mutant A56Y show similar activities in terms of binding to liposomes containing Gb_3 but differ dramatically with regard to affinity for P^k-glycoside and pentaSTARFISH (Table II). Our present results do not offer any explanation for this paradox. The only reasonable inference is that site 1 is more favorable for binding P^k trisaccharide displayed on membrane-localized glycolipid than in binding free trisaccharide. Unfortunately, direct, high resolution structural studies of the interaction of the B subunit with membrane-localized Gb_3 are not presently feasible.

The use of flow cytometry in combination with toxicity assays showed a logarithmic correlation between CD_{50} and VT1B binding to the cell surface for mutants with detectable binding, with the exception of W34A. In comparison to other mutants, the reduction in cell surface binding of W34A mutant was disproportionately large compared with the reduction in cytotoxicity. One of the features of W34A that distinguished it from other mutants was the slow dissociation of a population of the B pentamer molecules that bound to liposomal Gb_3, indicating a high avidity interaction. In fact, the dissociation rate constant of this population was virtually identical to that of the wild type. This probably reflects a correlation between dissociation rate and cytotoxicity. Our results demonstrated that disruption of individual sites had no influence on either the internalization rate or routing of bound toxin. It seems therefore that when the interaction is strong enough to bind toxin long enough for the initial contact to be effective, the following steps become determined and are independent of binding at specific sites on the B subunit.

The combination of the W34A mutation with the D17E or A56Y mutations reduced cytotoxicity 1000-fold further compared with the respective single site mutants. This is consistent with the ablation of liposome binding seen for the double mutants. Combined mutations at sites 1 and 2 produced a further 100- and 10-fold reduction in cytotoxicity compared with the single site mutants F30A and G62T, respectively, as would be expected if both sites were required for binding leading to cytotoxicity.

In summary, our data show marked differences between monovalent trisaccharide binding, pentavalent trisaccharide binding, and VT1 binding to membrane-localized Gb_3 and support the view that site 3 promotes homogeneous pentavalent binding at site 1 or 2. While site 2 has been shown to be the most favorable site for binding of monomeric P^k trisaccharide analogues, it is insufficient for high avidity binding of the B pentamer to membrane Gb_3. Thus the results strongly support

the view that all three VT1 oligosaccharide-binding sites are required for full biological activity and highlight the complexities and highly context-dependent nature of this protein-carbohydrate interaction. Our biological experiments also confirmed the validity of the liposomal model of the membrane-ligand interaction.

Acknowledgments—We thank R. J. Read and H. Ling for many helpful discussions and for providing structures prior to publication. We thank C. Lingwood, B. Boyd, and A. Nutikka for help in preparing glycolipids and generous donation of monoclonal antibody PH1. We thank Darrin Bast for preparing some of the mutant toxins.

REFERENCES

1. Riley, L., Remis, R., and Helgerson, S. (1983) *N. Engl. J. Med.* **308,** 681–685
2. Karmali, M. A., Petric, M., Lim, C., Cheung, R., and Arbus, G. (1985) *J. Infect. Dis.* **151,** 775–782
3. Endo, Y., Tsurugi, K., Yutsudo, T., Takeda, Y., Ogasavara, T., and Igarashi, K. (1988) *Eur. J. Biochem.* **171,** 45–50
4. Mangeney, M., Lingwood, C. A., Taga, S., Caillou, B., Tursz, T., and Wiels, J. (1993) *Cancer Res.* **53,** 5314–5319
5. Wadell, T., Cohen, A., and Lingwood, C. A. (1990) *Proc. Natl. Acad. Sci. U. S. A.* **87,** 7898–7901
6. Weinstein, D. L., Jackson, M. P., Perera, L. P., Holmes R. K., and O'Brien, A. D. (1989) *Infect. Immun.* **57,** 3743–3750
7. Donohue-Rolfe, A., Jacewicz, M., and Keusch, G. T. (1989) *Mol. Microbiol.* **3,** 1231–1236
8. Stein, P. E., Boodhoo, A., Tyrrell, G. J., Brunton, J. L., and Read, R. J. (1992) *Nature* **355,** 748–750
9. Ling, H., Boodhoo, A., Hazes, B., Cummings, M. D., Armstrong, G. D., Brunton, J. L., and Read, R. J. (1998) *Biochemistry* **37,** 1777–1788
10. Richardson, J. M., Evans, P. D., Homans, S. W., and Donohue-Rolfe, A. (1997) *Nat. Struct. Biol.* **4,** 190–193
11. Shimizu, H., Field, R. A., Homans, S. W., and Donohue-Rolfe, A. (1998) *Biochemistry* **37,** 11078–11082
12. Thompson, G. S., Shimizu, H., Homans, S. W., and Donohue-Rolfe, A. (2000) *Biochemistry* **39,** 13153–13156
13. Kitova, E. N., Kitov, P. I., Bundle, D. R., and Klassen, J. S. (2001) *Glycobiology* **11,** 605–611
14. Kitov, P. I., Sadowska, J. M., Mulvey, G., Armstrong, G. D., Ling, H., Pannu, N. S., Read, R. J., and Bundle, D. R. (2000) *Nature* **403,** 669–672
15. Bast, D. J., Banerjee, L., Clark, C., Read, R. J., and Brunton, J. L. (1999) *Mol. Microbiol.* **32,** 953–960
16. MacKenzie, C. R., Hirama, T., Lee, K. K., Altman, E., and Young, N. M. (1997) *J. Biol. Chem.* **272,** 5533–5538
17. Basta, M., Karmali, M., and Lingwood, C. (1989) *J. Clin. Microbiol.* **127,** 1617–1622
18. Boyd, B., Richardson, S., and Gariepy, J. (1991) *Infect. Immun.* **59,** 750–757
19. Kihlberg, J., Hultgren, S. J., Normark, S., and Magnusson, G. (1989) *J. Am. Chem. Soc.* **111,** 6364–6368
20. Stockbine, N. A., Marques, L. R. M., Newland, J. W., Smith, H. W., Holmes, R. K., and O'Brien, A. D. (1985) *Infect. Immun.* **53,** 135–140
21. Messing, J., Crea, R., and Seeburg, P. H. (1981) *Nucleic Acids Res.* **9,** 309–321
22. Kunkel, T. A. (1987) *Methods Enzymol.* **154,** 367–383
23. Ramotar, K., Boyd, B., Tyrell, G., Gariepy, J., Lingwood, C. A, and Brunton, J. (1990) *Biochem. J.* **272,** 805–811
24. Petric, M., Karmali, M. A., Richardson, S. E., and Cheung, R. (1987) *FEMS Microbiol. Lett.* **41,** 63–68
25. Clark, C., Bast, D., Sharp, A. M., St. Hilaire, P., Agha, R., Stein, P. E., Toone, E. J., Read, R. J., and Brunton, J. L. (1996) *Mol. Microbiol.* **19,** 891–899
26. Davies, G., and Stark, G. (1970) *Proc. Natl. Acad. Sci. U. S. A.* **66,** 651–656
27. Jönsson, U., Fägerstam, L., Ivarsson, B., Johnsson, B., Karlsson, R., Lundh, K., Löfås, S., Persson, B., Roos, H., Rönnberg, I., Sjölander, S., Stenberg, E., Ståhlberg, R., Urbaniczky, C., Östlin, H., and Malmqvist, M. (1991) *BioTechniques* **11,** 620–627
28. Lingwood, C. A., Law, H., Richardson, S., Petric, M., Brunton, J. L., De Grandis, S., and Karmali, M. (1987) *J. Biol. Chem.* **262,** 8834–8839
29. Khine, A. A., and Lingwood, C. A. (1994) *J. Cell. Physiol.* **161,** 319–332
30. Schapiro, F. B., Lingwood, C. A., Furuya, W., and Grinstein. S. (1998) *Am. J. Physiol.* **274,** C319-C332
31. Kiarash, A., Boyd, B., and Lingwood, C. A. (1994) *J. Biol. Chem.* **269,** 11138–11146
32. Pellizari, A., Pang, H., and Lingwood, C. A. (1992) *Biochemistry* **31,** 1363–1370
33. Fuchs, G., Mobassaleh, M., Donohue-Rolfe, A., Montgomery, R., Gerard, R., and Keush, G. (1986) *Infect. Immun.* **53,** 372–378
34. Head, S. C., Karmali, M. A., and Lingwood, C. A. (1991) *J. Biol. Chem.* **266,** 3617–3621
35. Nakajima, H., Kiyokawa, N., Katagiri, Y. U., Taguchi, T., Suzuki, T., Sekino, T., Mimori, K., Ebata, T., Saito, M., Nakao, H., Takeda, T., and Fujimoto, J. (2001) *J. Biol. Chem.* **276,** 42915–42922
36. Picking, W. D., McCann, J. A., Nutikka, A., and Lingwood, C. A. (1999) *Biochemistry* **38,** 7177–7184
37. Ling, H. (1999) *Structural Studies of the Interactions between Shiga-like Toxins and Their Carbohydrate Receptor*. Ph.D. thesis, University of Alberta, Alberta, Canada
38. Sharp, A. (2000) *Structural Studies of Active Plasminogen Activator Inhibitor-1 and Shiga-like Toxin-1.* Ph.D. thesis, University of Alberta, Alberta, Canada

A Mutational Analysis of the Globotriaosylceramide-binding Sites of Verotoxin VT1

Anna M. Soltyk, C. Roger MacKenzie, Vince M. Wolski, Tomoko Hirama, Pavel I. Kitov, David R. Bundle and James L. Brunton

J. Biol. Chem. 2002, 277:5351-5359.
doi: 10.1074/jbc.M107472200 originally published online November 26, 2001
